Research Article

Solid lipid nanoparticles loading with curcumin and dexanabinol to treat major depressive disorder

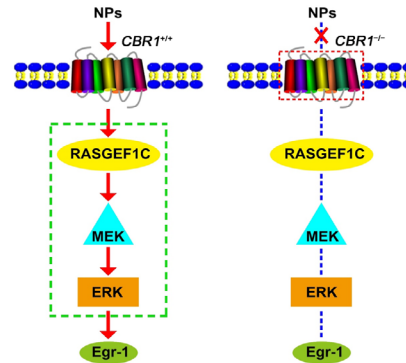Xiao-Lie He, Li Yang, Zhao-Jie Wang, Rui-Qi Huang, Rong-Rong Zhu*, Li-Ming Cheng*

Graphical Abstract *Schematic representation of the reason why functionalized solid lipid nanoparticles (NPs) loading with curcumin and dexanabinol behave differently in CBR1⁺/⁺ and CBR1⁻/⁻ major depressive disorder mice*

Abstract

Dexanabinol (HU-211) is an artificially synthesized cannabinoid derivative that exerts neuroprotective effects through anti-inflammatory and antioxidant effects. Curcumin exhibits antidepressant effects in the treatment of major depressive disorder. To investigate the antidepressant effects of solid lipid nanoparticles loaded with both curcumin and dexanabinol, and the underlying mechanisms associated with this combination, we established wild-type ($CBR1^{+/+}$) and cannabinoid receptor 1 (CBR1) knockout ($CBR1^{-/-}$) mouse models of major depressive disorder, through the intraperitoneal injection of corticosterone, for 3 successive days, followed by treatment with intraperitoneal injections of solid lipid nanoparticles loading with curcumin (20 mg/kg) and dexanabinol (0.85 mg/kg), for 2 successive days. Our results revealed that solid lipid nanoparticle loading with curcumin and dexanabinol increased the mRNA and protein expression levels of the mature neuronal markers neuronal nuclei, mitogen-activated protein 2, and neuron-specific beta-tubulin III, promoted the release of dopamine and norepinephrine, and increased the mRNA expression of CBR1 and the downstream genes *Rasgef1c* and *Egr1*, and simultaneously improved rat locomotor function. However, solid lipid nanoparticles loaded with curcumin and dexanabinol had no antidepressant effects on the $CBR1^{-/-}$ mouse models of major depressive disorder. This study was approved by the Institutional Ethics Committee of Tongji Hospital of Tongji University, China (approval No. 2017-DW-020) on May 24, 2017.

Key Words: biocompatibility; curcumin; depression; dexanabinol; dopamine; nanoparticles; norepinephrine

Chinese Library Classification No. R453; R749.4; R318

Introduction

Major depressive disorder (MDD) is a common mood disturbance syndrome, characterized primarily by a general loss of interest in life, for at least 2 weeks (Boku et al., 2018; Seki et al., 2018). Selective serotonin reuptake inhibitors are frequently used to treat MDD; however, the long-term uptake of selective serotonin reuptake inhibitors may induce high toxicity, negating their beneficial effects (Amare et al., 2019). Ongoing studies have been performed to identify new antidepressant treatments for MDD.

Cannabinoid receptor 1 (CBR1) is primarily expressed in the peripheral and central nervous systems. The endocannabinoid system that acts on CBR1 is involved in the regulation of human emotions and has been associated with depression (Zhou et al., 2017). At the preclinical level, the misregulation of the endocannabinoid pathway has been associated with a depression-like phenotype (Hill et al., 2008). Significantly reduced CBR1 mRNA expression levels have been demonstrated in the blood of MDD patients compared with the normal population (Lakiotaki et al., 2015). CBR1 agonists can enhance central neurotransmitter delivery and facilitate hippocampal neurogenesis and share mechanisms with other antidepressants (Bambico and Gobbi, 2008). According to previous studies, cannabidiol, which is a potent CBR1 antagonist, and the central CBR1 agonist dexanabinol (HU-211) exerted dose-dependent antidepressant-like effects during the forced-swim test (FST), in rodent models of depression, similar

Key Laboratory of Spine and Spinal Cord Injury Repair and Regeneration of Ministry of Education, Department of Orthopedics, Tongji Hospital, School of Life Science and Technology, Tongji University, Shanghai, China

*Correspondence to: Li-Ming Cheng, limingcheng@tongji.edu.cn; Rong-Rong Zhu, rrzhu@tongji.edu.cn.
https://orcid.org/0000-0003-3396-4300 (Li-Ming Cheng); https://orcid.org/0000-0002-3955-5965 (Rong-Rong Zhu)

to known antidepressant drugs (El-Alfy et al., 2010). Activated CBR1 can prevent the development of depressive symptom patterns of emotional learning in rat models of chronic mild stress (Segev et al., 2014). Another study revealed that CBR1 ligands can strengthen the antidepressant effects of bioactive metals (i.e., 10 mg/kg magnesium or 5 mg/kg zinc) (Wośko et al., 2018).

HU-211 is an artificially synthesized cannabinoid derivative, which has been demonstrated to exert neuroprotective effects, anti-inflammatory, and antioxidant activities (Durmaz et al., 2008). Curcumin (Cur) has also demonstrated antidepressant effects against major depression (Kalani and Chaturvedi, 2017; Chen et al., 2018). Nanoparticles (NPs), especially solid-lipid NPs, have demonstrated great potential for the treatment of MDD (Andrade et al., 2016; Dening et al., 2016), and functionalized, solid-lipid NPs, loaded with Cur and HU-211 (Cur/SLNs-HU-211) and capable of targeting CBR1, have been regarded as a potential antidepressant treatment strategy (He et al., 2016). Lipid NPs may be advantageous for dual-drug loading and antioxidant delivery for the following reasons: 1) encapsulated biomolecules demonstrate excellent bioavailability; 2) encapsulated substances, including therapeutic macromolecules, demonstrate sustained release; 3) lipid NPs can encapsulate and transport both lipophilic and hydrophilic drugs; 4) lipid NPs show a high encapsulation efficacy for guest molecules; 5) lipid NPs have biodegradable and biocompatible properties; and 6) lipid NPs represent non-toxic carriers. In our previous studies, solid-lipid NPs were employed to overcome the poor solubility, stability, and bioavailability of Cur and HU-211, promoting their utilization in PD (Guerzoni et al., 2017; Rakotoarisoa and Angelova, 2018; Rakotoarisoa et al., 2019).

Therefore, in this study, we examined a corticosterone (CORT)-induced MDD mouse model, to more precisely understand the role played by Cur/SLNs-HU-211 in wild-type ($CBR1^{+/+}$) and CBR1 knockout ($CBR1^{-/-}$) mice. We performed a behavioral test, detected neurotransmitter levels, and analyzed neural marker expression and transcriptome sequencing, to identify the functions of Cur/SLNs-HU-211.

Materials and Methods

Preparation of Cur/SLNs-HU-211 and $CBR1^{-/-}$ mice

Cur/SLNs-HU-211 was composited, as described previously (He et al., 2017). In brief, 0.15 g Cur (Aladdin, Shanghai, China), 0.2 g stearic acid (Sigma, Darmstadt, Germany), 0.1 g lecithin (Sigma), and 0.002 g HU-211 (Cayman Chemical, Ann Arbor, MI, USA) were dissolved in 10 mL chloroform and then added into 30 mL H_2O, containing 0.25 g Myrj52 (Sigma). The mixture was stirred at 1200 r/min at 75°C, for 1 hour. Cold water (10 mL) was added, and the mixture was stirred for an additional 2 hours, at 4°C. Then, the mixture was centrifuged at 4°C for 2 hours at 20,000 r/min, to collect the NPs. All materials used in this process were analytical grade.

Twenty-four female $CBR1^{+/+}$ and 24 female $CBR1^{-/-}$ mice, aged 8 weeks, were obtained from Bioray Laboratories Inc. [Shanghai, China; license No. SCXK (Hu) 2016-0004] and raised at the Laboratory Animal Centre of Tongji Hospital of Tongji University, China. These experiments were authorized by the Institutional Research Ethics Committee of Tongji Hospital of Tongji University, China (approval No. 2017-DW-020) on May 24, 2017, and strictly followed the National Institutes of Health Guide for the Use and Care of mice.

Mice were genotyped using a Direct Mouse Genotyping Kit, acquired from APExBIO Technology (Houston, TX, USA), and the mice were randomly assigned to six groups (n = 8/group): (1) $CBR1^{+/+}$ mice injected with 100 μL normal saline; (2) $CBR1^{+/+}$ mice injected with 100 μL CORT (solubilized in 10% DMSO and 90% corn oil) only; (3) $CBR1^{+/+}$ mice injected with 100 μL CORT and 100 μL Cur/SLNs-HU-211 (solubilized in sterilized water);

(4) $CBR1^{-/-}$ mice injected with 100 μL normal saline; (5) $CBR1^{-/-}$ mice injected with CORT only; and (6) $CBR1^{-/-}$ mice injected with CORT and Cur/SLNs-HU-211.

A mouse model of depression was generated by the intraperitoneal injection of CORT (40 mg/kg per day), for 21 days (Gregus et al., 2005). Cur/SLNs-HU-211 was administered for 2 weeks, at a Cur concentration of 20 mg/kg per day, and an HU-211 concentration of 0.85 mg/kg per day, by intraperitoneal injection following the 21-day CORT intervention. The experimental process is shown in **Figure 1A**. Hippocampal and striatum samples from each group were used to confirm the genotypes of $CBR1^{+/+}$ and $CBR1^{-/-}$ mice.

Behavioral tests

To assess motor functional recovery, the mice were subjected to the FST, 2 days after the end of the entire 2-week drug-administration period, and to the pole test, 3 days after drug administration (Aguiar et al., 2020; Hou et al., 2020; Szczepanik et al., 2020). For the FST, mice were dropped into a beaker containing water, and their behaviors were recorded. During the final 6 minutes of an 8-minute test, the float time was calculated. During the pole test, mice are placed at the top of a pole (0.8 cm in diameter; 60 cm in height) and the time spent climbing down the pole was measured. All experiments were performed three times.

Dopamine and norepinephrine detection

Mice hippocampus and striatum samples were collected 4 days after drug administration. Samples were immersed in 400 μL phosphate-buffered saline, homogenized, mixed with 800 μL acetonitrile, and centrifuged at 4°C for 15 minutes at 12,000 r/min, to obtain the supernatant. Sample volumes equal to 20 μL were injected onto high-performance liquid chromatography columns (Agilent, Santa Clara, CA, USA). The mobile phase consisted of 10% methanol and 90% 0.01 M KH_2PO_4 (pH 3.5), at a flow rate of 500 μL/min. The concentrations of dopamine (DA) were measured at 280 nm, using a microplate reader (Thermo Fisher Scientific Inc., Waltham, MA, USA). For the detection of norepinephrine (NE), the mobile phase consisted of 60% methanol and 40% 0.05 M CH_3COONa, and a detection wavelength of 275 nm was applied. The protein concentrations were quantified by a BCA Kit (Keygen, Nanjing, China).

Quantitative reverse transcription-polymerase chain reaction

Quantitative reverse transcription-polymerase chain reaction (qRT-PCR) was performed, in accordance with standard protocols, 4 days after drug administration (Kroh et al., 2010). Total RNA was extracted from hippocampal and striatum samples using TRIZol reagent (Takara, Dalian, China), and complementary DNA was obtained using a PrimeScript RT reagent kit (Takara). qRT-PCR was performed using SYBR Green (Takara). Glyceraldehyde 3-phosphate dehydrogenase was used as an internal reference, forward primer: 5′-GTG TTC CTA CCC CCA ATG TGT-3′; reverse primer: 5′-ATT GTC ATA CCA GGA AAT GAG CTT-3′. The primer sequences used were as follows: NeuN, forward primer: 5′-ATC GTA GAG GGA CGG AAA ATT GA-3′; reverse primer: 5′-GTT CCC AGG CTT CTT ATT GGT C-3′; microtubule-associated protein 2 (*Map2*), forward primer: 5′-GCC AGC CTC AGA ACA AAC AG-3′; reverse primer: 5′-AAG GTC TTG GGA GGG AAG AAC-3′; class III β-tubulin (*Tuj1*), forward primer: 5′-TAG ACC CCA GCG GCA ACT AT-3′; reverse primer: 5′-GTT CCA GGT CCA AGT CC ACC-3′; *CBR1*, forward primer: 5′-AAG TCG ATC TTA GAC GGC CTT-3′; reverse primer: 5′-TCC TAA TTT GGA TGC CAT GTC TC-3′; RasGEF domain family member 1C (*Rasgef1c*), forward primer: 5′-TGC CCA CAG CCG ATT ACT ATC-3′; reverse primer: 5′-CAC AGG TGA CAC ACC CGA G-3′; and early growth response 1 (*Egr1*), forward primer: 5′-TCG GCT CCT TTC CTC ACT CA-3′; reverse primer: 5′-CTC ATA GGG TTG TTC GCT CGG-3′.

Western blot assay

Western blot assays were performed on the hippocampus and striatum protein samples, using a standard protocol (Burnette, 1981). Samples were mixed with 5× sodium dodecyl sulfate-polyacrylamide gel electrophoresis loading buffer and boiled at 95°C for 5 minutes. Samples containing 20 µg protein were loaded in each lane, separated by sodium dodecyl sulfate-polyacrylamide gel electrophoresis, and then transferred to a polyvinylidene difluoride membrane. The membrane was blocked with 5% (w/v) bovine serum albumin and incubated with the specific primary antibodies. Antibodies specific to NeuN (Cat# ab104225; 1:5000; rabbit; Abcam, Cambridge, MA, USA), MAP2 (Cat# ab11267; 1:1000; mouse; Abcam), Tuj1 (Cat# ab78078; 1:1000; mouse; Abcam), CBR1 (Cat# ab23703; 1:200; rabbit; Abcam), RASGEF1C (Cat# abs139329; 1:1000; rabbit; Absin, Shanghai, China), mitogen-activated protein kinase kinase (MEK; Cat# ab32091; 1:1000; rabbit; Abcam), phospho (p)-MEK (Cat# ab214445; 1:1000; rabbit; Abcam), extracellular signal-regulated kinase (ERK; Cat# ab184699; 1:2000; rabbit; Abcam), p-ERK (Cat# ab32538; 1:1000; rabbit; Abcam), Egr1 (Cat# ab133695 1:1000; rabbit; Abcam), and β-actin (Cat# bsm-33036M; 1:1000; mouse; Bioss, Woburn, MA, USA) were used. Membranes were incubated with primary antibodies overnight at 4°C. The membrane was incubated with mouse or rabbit second antibodies, conjugated to horseradish peroxidase (Cat# 7076/7074; 1:1000; CST, Danvers, MA, USA), for 1 hour at room temperature, and then detected using a chemiluminescence detection system (GE, Boston, MA, USA). Images were further analyzed by Photoshop CS6 (Adobe, San Jose, CA, USA).

Immunofluorescence

Immunofluorescence analysis was performed using standard protocols (Liu et al., 2020). After 4% paraformaldehyde fixation, 10-µm sections from the hippocampus and striatum were washed twice with phosphate-buffered saline and permeated using 0.2% Triton X-100 for 15 minutes. The sections were blocked with blocking buffer (normal goat serum and 0.3% Triton X-100 in phosphate-buffered saline), for 1 hour at room temperature, and incubated with primary antibody against NeuN (Cat# ab104225; 1:500; rabbit; Abcam), overnight at 4°C. Subsequently, sections were incubated with appropriate fluorescently tagged secondary antibodies, at 1:200 (Alexa Fluor® 488 AffiniPure goat anti-rabbit antibody; Yeasen, Shanghai, China) for 1 hour at room temperature, and 4′,6-diamidino-2-phenylindole (Sigma) was used. Finally, the samples were observed under a fluorescence microscope (Leica, Wetzlar, Germany).

Bioinformatics analysis

Total RNAs were isolated from the hippocampus and then RNA sequencing libraries were generated. Transcriptome sequencing was performed on a BGISEQ-500 system at BGI Company (Shenzhen, China), and the sequences were analyzed using 2-dimensional (2D) principal component analysis and Kyoto Encyclopedia of Genes and Genomes (KEGG) annotation.

Statistical analysis

Experimental results are presented as the mean ± standard deviation (SD). A one-way analysis of variance was performed for each analysis, and the least significant difference test was used for further intergroup comparisons. $P < 0.05$ was considered significant. All data were analyzed using SPSS 17.0 software (IBM Corp., Armonk, NY, USA).

Results

Identification of mouse genotype

As shown by the schematic (**Figure 1A**), both wild-type ($CBR1^{+/+}$) and $CBR1^{-/-}$ mice were treated with CORT and Cur/SLNs-HU-211, and experiments were performed to determine whether NPs exert beneficial effects in CORT-treated $CBR1^{+/+}$ and $CBR1^{-/-}$ mice. Mouse hippocampus and striatum samples from all six groups were collected, and the genotype of each mouse was identified. qRT-PCR amplification was performed on a thermal cycler, yielding an 804-bp fragment from homozygous $CBR1^{+/+}$ mice and a 628-bp fragment from homozygous $CBR1^{-/-}$ mice (**Figure 1B**), which confirmed that the $CBR1^{-/-}$ mice were CBR1-deficient.

Cur/SLNs-HU-211 improves motor function and neurotransmitter expression in MDD mice

Mice behavioral tests can represent useful tools for evaluating the curative effects of drugs. In our study, we used the FST and pole test to evaluate mouse motor functional improvements. The FST results suggested that Cur/SLNs-HU-211 treatment greatly improved the float time in CORT-treated $CBR1^{+/+}$ mice, from 36.5 seconds in mice treated with CORT alone to 46.5 seconds in mice treated with both CORT and Cur/SLNs-HU-211 ($P = 0.026$); however, no such improvement was observed in $CBR1^{-/-}$ mice ($P = 0.539$) (**Figure 1C**). To measure bradykinesia, we implemented the pole test, and the results showed that mice in the CORT group took longer to climb down the pole than mice in the control group ($P = 0.023$; **Figure 1D**). Treatment with Cur/SLNs-HU-211 significantly reduced the climbing times compared with those for the CORT alone group, in $CBR1^{+/+}$ mice (8.7 seconds $vs.$ 11.3 seconds, $P = 0.047$), indicating that they descended much faster. In $CBR1^{-/-}$ mice, no significant difference was observed in climbing time between the CORT alone and the CORT + Cur/SLNs-HU-211 groups ($P = 0.751$). These results demonstrated that Cur/SLNs-HU-211 treatment could effectively reverse CORT-induced motor deficits in $CBR1^{+/+}$ mice but not $CBR1^{-/-}$ mice.

High-performance liquid chromatography was used to detect DA and NE levels in the hippocampus and striatum samples. As shown in **Figure 1E** and **G**, DA levels in the hippocampus and striatum were reduced after CORT administration ($P = 0.027$ and 0.001, respectively). In $CBR1^{-/-}$ mice, Cur/SLNs-HU-211-treated animals exhibited no changes in DA levels in the hippocampus and striatum compared with those in the CORT group ($P = 0.193$ and 0.017, respectively). For $CBR1^{+/+}$ mice, Cur/SLNs-HU-211 treatment remarkably enhanced DA release in CORT-treated mice, for both the hippocampus and striatum ($P = 0.033$ and 0.002, respectively). NE levels were also measured (**Figure 1F** and **H**). CORT treatment induced significant decreases in NE levels in both the hippocampus and striatum ($P = 0.002$ and 0.008, respectively), and this decrease can be reversed by Cur/SLNs-HU-211 treatment in $CBR1^{+/+}$ mice ($P = 0.002$ and 0.001, respectively). In $CBR1^{-/-}$ MDD model mice, Cur/SLNs-HU-211 induced no significant effects on NE levels in the hippocampus and striatum ($P = 0.702$ and 0.377, respectively). The recovery of DA and NE levels observed for Cur/SLNs-HU-211 treatment in $CBR1^{+/+}$ MDD mice indicated that Cur/SLNs-HU-211 could significantly elevate the levels of monoamine neurotransmitters in MDD mice. The lack of recovery in $CBR1^{-/-}$ mice indicated that this recovery is CBR1-dependent.

Cur/SLNs-HU-211 promotes neural differentiation in hippocampus and striatum of MDD mice

To study the impact of Cur/SLNs-HU-211 treatment on the expression patterns of NeuN, MAP2, and Tuj1, a western blot assay was performed. The protein expression levels of the mature neuronal markers NeuN, MAP2, and Tuj1 were significantly increased in Cur/SLNs-HU-211-treated $CBR1^{+/+}$ MDD model mice (**Figure 2A**). In Cur/SLNs-HU-211-treated $CBR1^{-/-}$ MDD model mice, no changes were observed compared with untreated $CBR1^{-/-}$ MDD model mice.

We analyzed the expression of neuron-specific genes (*NeuN*, *Map2*, and *Tuj1*). The qRT-PCR analysis showed that the mRNA levels of *NeuN*, *Map2*, and *Tuj1* in hippocampus (*NeuN*:
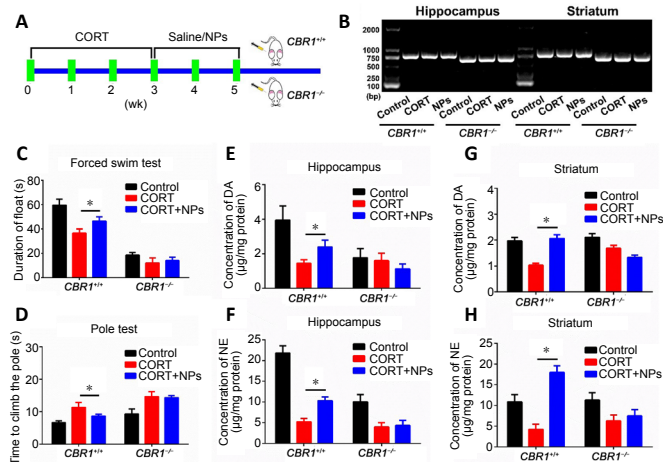
Figure 1 | Experiment design, motor function recovery, and neurotransmitter detection.
(A) Flow chart showing MDD model establishment and drug administration in $CBR1^{+/+}$ and $CBR1^{-/-}$ mice. For the first 3 weeks, CORT was administered to generate an MDD animal model. Then, saline or Cur/SLNs-HU-211 were administered for the next 2 weeks. (B) CBR1 bands for genotype identification of $CBR1^{+/+}$ and $CBR1^{-/-}$ mice, in hippocampus and striatum samples, to ensure the proper mouse classification. (C) Float time in the FST. Mice were placed in water, and the floating or swimming behavior was measured as an indicator of depressive behaviors. (D) The time taken to climb the pole during the pole test. Mice were placed at the top of a pole, and healthier animals tended to climb down more quickly. (E, F) Concentrations of DA (E) and NE (F) in the hippocampus. (G, H) Concentrations of DA (G) and NE (H) in the striatum. Data are presented as the mean ± SD (n = 3/group). *P < 0.05 (one-way analysis of variance, followed by the least significant difference test). $CBR1^{-/-}$: Cannabinoid receptor 1 knockout; $CBR1^{+/+}$: wild-type; CORT: corticosterone; DA: dopamine; FST: forced-swim test; MDD: major depressive disorder; NE: norepinephrine; NPs: nanoparticles loaded with curcumin and dexanabinol (Cur/SLNs-HU-211).

P = 0.005; $Map2$: P = 0.012; $Tuj1$: P = 0.006) and striatum ($NeuN$: P = 0.029; $Map2$: P = 0.018; $Tuj1$: P = 0.028) were reduced significantly in MDD model mice following CORT injection, compared with those in the control group (**Figure 2B**). After the administration of Cur/SLNs-HU-211, the levels of $NeuN$, $Map2$, and $Tuj1$ mRNA in the hippocampus ($NeuN$: P = 0.024; $Map2$: P = 0.023; $Tuj1$: P = 0.026) and striatum ($NeuN$: P = 0.035; $Map2$: P = 0.033; $Tuj1$: P = 0.006) increased significantly, relative to those in untreated $CBR1^{+/+}$ MDD model mice. In contrast, in $CBR1^{-/-}$ MDD model mice, Cur/SLNs-HU-211 treatment was unable to promote increases in these mRNA levels in the hippocampus ($NeuN$: P = 0.724; $Map2$: P = 0.435; $Tuj1$: P = 0.751) and striatum ($NeuN$: P = 0.36; $Map2$: P = 0.004; $Tuj1$: P = 0.334). These results demonstrated that Cur/SLNs-HU-211 can only benefit $CBR1^{+/+}$ MDD model mice, by increasing NeuN, $Map2$, and $Tuj1$ mRNA levels in the hippocampus and striatum.

To analyze neuronal survival, we examined NeuN expression, as a neuronal biomarker (**Figure 2C**). Compared with both the $CBR1^{+/+}$ and $CBR1^{-/-}$ control groups, CORT administration resulted in neuronal cell death, and few NeuN-positive cells were found in the hippocampus and striatum of MDD model mice. However, more NeuN-positive neurons were observed in $CBR1^{+/+}$ MDD model mice following treatment with Cur/SLNs-HU-211, whereas fewer NeuN-positive cells were detected in $CBR1^{-/-}$ MDD model mice following Cur/SLNs-HU-211 treatment.

Molecular mechanisms of Cur/SLNs-HU-211 on neural differentiation in MDD model mice
To explore the underlying molecular mechanisms in more detail, we employed transcriptome sequencing to examine differential gene expression among our experimental groups, to reveal the *in vivo* working systems. A heatmap, showing the mRNA expression profiles of all samples, can be observed

in **Figure 3A**. A total of 505 differentially expressed genes were identified between the $CBR1^{+/+}$ CORT + Cur/SLNs-HU-211 and the CORT alone groups. We listed the 17 most-relevant genes in **Figure 3B**, most of which are associated with neurodevelopment. The two-dimensional principal component analysis for all samples and all genes separated the CORT + Cur/SLNs-HU-211 ($CBR1^{-/-}$) group the farthest from the control ($CBR1^{+/+}$) group, whereas the CORT + Cur/SLNs-HU-211 ($CBR1^{+/+}$) group was the closest (**Figure 3C**). We recognized eight related Kyoto Encyclopedia of Genes and Genomes pathways in the $CBR1^{+/+}$ CORT + Cur/SLNs-HU-211 and CORT alone groups (**Figure 3D**). Among pathways with significant differences, we focused on the mitogen-activated protein kinase pathway because the mitogen-activated protein kinase has been reported to play a vital role in MDD (Bruchas et al., 2011; Yamamoto et al., 2012). We then examined these genes by qRT-PCR and western blot assays. The qRT-PCR results showed that in Cur/SLNs-HU-211-treated $CBR1^{+/+}$ MDD model mice, $CBR1$, $Rasgef1c$, and $Egr1$ mRNA expression increased compared with untreated $CBR1^{+/+}$ MDD model mice in the hippocampus ($CBR1$: P = 0.01; $Rasgef1c$: P = 0.02; $Egr1$: P = 0.03) and striatum ($CBR1$: P = 0.005; $Rasgef1c$: P = 0.003; $Egr1$: P = 0.001), whereas Cur/SLNs-HU-211-treated $CBR1^{-/-}$ MDD model mice showed no significant increase in mRNA expression in the hippocampus ($CBR1$: P = 0.001; $Rasgef1c$: P = 0.096; $Egr1$: P = 0.052) and striatum ($CBR1$: P = 0.636; $Rasgef1c$: P = 0.466; $Egr1$: P = 0.451) compared with untreated $CBR1^{-/-}$ MDD model mice (**Figure 3E**). We further used western blotting analysis to investigate the corresponding protein expression levels of CBR1, RASGEF1C, and Egr1, in addition to the phosphorylation of MEK and ERK, all of which were up-regulated in Cur/SLNs-HU-211-treated $CBR1^{+/+}$ MDD model mice compared with untreated $CBR1^{+/+}$ MDD model mice; however, no significant changes were observed in $CBR1^{-/-}$ mice (**Figure 3F**). The total protein levels of MEK and ERK were observed to be similar among all groups.

Discussion
MDD is currently the only disease in which curcumin has been recognized to serve as a putative therapeutic agent, through clinical trials. However, more research remains necessary to address existing problems associated with curcumin, including relatively low solubility, poor oral bioavailability, and instability (Lopresti, 2017). Dexanabinol exerts potent protective effects during trauma and ischemia; however, instability and poor absorption have limited its application (Darlington, 2003). The Cur/SLNs-HU-211 examined in this study were employed to overcome these barriers to the applications of curcumin and dexanabinol for therapeutic purposes.

CBR1 has previously been implicated in the regulation of MDD. Rimonabant, a CBR1 antagonist used to treat obesity is associated with an increased risk of severe depression (Christensen et al., 2007). In contrast, the administration of synthetic cannabinoids in the NAc has been demonstrated to produce antidepressant-like effects (Shen et al., 2019). Nanoparticles represent a potential and readily available tool for the targeted delivery of antidepressant drugs. Melatonin-loaded nanoparticles displayed better antidepressant activity compared with that of free melatonin (Si et al., 2020). The antidepressant-like effects of silymarin, especially in nanoparticle form have been associated with antioxidant and anti-inflammatory effects (Ashraf et al., 2019).

In this study, we found that the MAPK pathway was involved in the neuroprotective effects exerted by Cur/SLNs-HU-211, which was regulated by the enhanced expression of RASGEF1C/Egr1, and this entire process was mediated by CBR1. Previous studies have also implied that the activation of CBR1 modulated the phosphorylation status of ERK1/2 (López-Cardona et al., 2017). Together, these findings suggested that
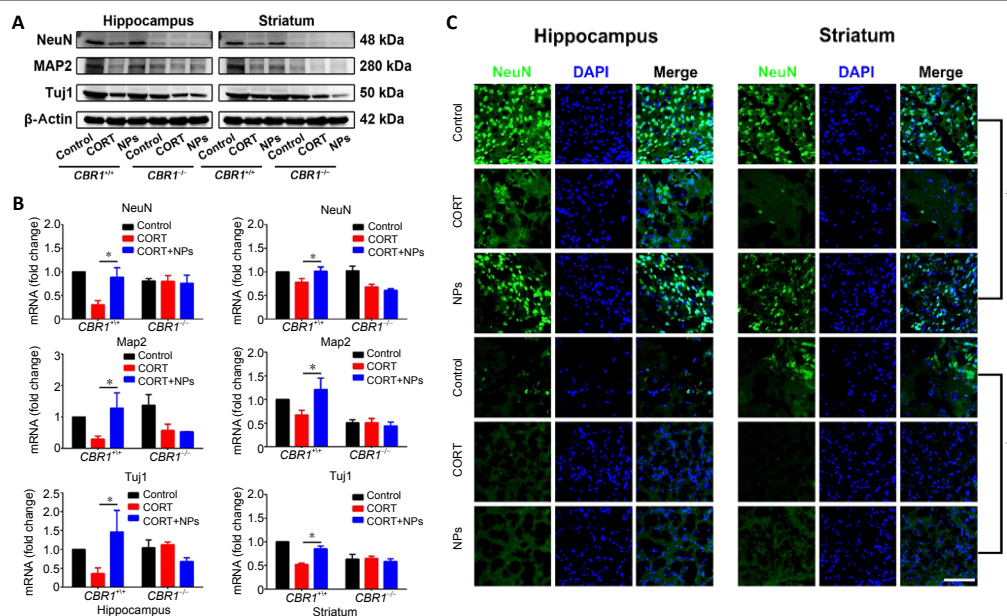
Figure 2 │ **Effects of Cur/SLNs-HU-211 on the expression levels of neuronal markers in *CBR1*^+/+^ and *CBR1*^−/−^ MDD model mice.**
(A) Western blot images showing the NeuN, MAP2, and Tuj1 levels in the hippocampus and striatum. (B) Quantitative reverse transcription-polymerase chain reaction analysis of NeuN, MAP2, and Tuj1 mRNA levels in the hippocampus and striatum. mRNA expression levels were normalized against GAPDH expression levels in the *CBR1*^+/+^ control group. Data are presented as the mean ± SD (*n* = 3/group). *$P < 0.05$ (one-way analysis of variance, followed by the least significant difference test). (C) Representative immunofluorescence images of NeuN-positive cells (green, stained by Alexa Fluor® 488), in the hippocampus and striatum. Scale bar: 100 μm. *CBR1*^−/−^: Cannabinoid receptor 1 knockout; *CBR1*^+/+^: wild-type; CORT: corticosterone; Cur/SLNs-HU-211: solid-lipid nanoparticles loaded with curcumin and dexanabinol; DAPI: 4′,6-diamidino-2-phenylindole; GAPDH: glyceraldehyde 3-phosphate dehydrogenase; MAP2: microtubule-associated protein 2; MDD: major depressive disorder; NPs: nanoparticles loaded with curcumin and dexanabinol (Cur/SLNs-HU-211); Tuj1: class III β-tubulin.

MDD improvements may be closely linked to the regulation of the CBR1 and MAPK pathway.

Our findings suggested that CBR1 is necessary for the effects observed in response to Cur/SLNs-HU-211 treatment; however, the current study has some limitations. The formed nanoparticles require optimization to enhance their performance, and the biocompatibility of nanoparticles should be investigated carefully. Furthermore, the use of a conditional knockout CBR1 animal model would represent a better model to study the effects of these nanoparticles. Future work should address these issues to provide a novel medicinal strategy for the treatment of MDD and other neurodegenerative diseases in clinical practice.

References

Aguiar RP, Soares LM, Meyer E, da Silveira FC, Milani H, Newman-Tancredi A, Varney M, Prickaerts J, Oliveira RMW (2020) Activation of 5-HT(1A) postsynaptic receptors by NLX-101 results in functional recovery and an increase in neuroplasticity in mice with brain ischemia. Prog Neuropsychopharmacol Biol Psychiatry 99:109832.

Amare AT, Schubert KO, Tekola-Ayele F, Hsu YH, Sangkuhl K, Jenkins G, Whaley RM, Barman P, Batzler A, Altman RB, Arolt V, Brockmöller J, Chen CH, Domschke K, Hall-Flavin DK, Hong CJ, Illi A, Ji Y, Kampman O, Kinoshita T, et al. (2019) The association of obesity and coronary artery disease genes with response to SSRIs treatment in major depression. J Neural Transm (Vienna) 126:35-45.

Andrade PB, Grosso C, Valentao P, Bernardo J (2016) Flavonoids in neurodegeneration: limitations and strategies to cross CNS barriers. Curr Med Chem 23:4151-4174.

Ashraf A, Mahmoud PA, Reda H, Mansour S, Helal MH, Michel HE, Nasr M (2019) Silymarin and silymarin nanoparticles guard against chronic unpredictable mild stress induced depressive-like behavior in mice: involvement of neurogenesis and NLRP3 inflammasome. J Psychopharmacol 33:615-631.

Bambico FR, Gobbi G (2008) The cannabinoid CB1 receptor and the endocannabinoid anandamide: possible antidepressant targets. Expert Opin Ther Targets 12:1347-1366.

Boku S, Nakagawa S, Toda H, Hishimoto A (2018) Neural basis of major depressive disorder: beyond monoamine hypothesis. Psychiatry Clin Neurosci 72:3-12.

Bruchas MR, Schindler AG, Shankar H, Messinger DI, Miyatake M, Land BB, Lemos JC, Hagan CE, Neumaier JF, Quintana A, Palmiter RD, Chavkin C (2011) Selective p38α MAPK deletion in serotonergic neurons produces stress resilience in models of depression and addiction. Neuron 71:498-511.

Burnette WN (1981) "Western blotting": electrophoretic transfer of proteins from sodium dodecyl sulfate--polyacrylamide gels to unmodified nitrocellulose and radiographic detection with antibody and radioiodinated protein A. Anal Biochem 112:195-203.

Chen M, Du ZY, Zheng X, Li DL, Zhou RP, Zhang K (2018) Use of curcumin in diagnosis, prevention, and treatment of Alzheimer's disease. Neural Regen Res 13:742-752.

Christensen R, Kristensen PK, Bartels EM, Bliddal H, Astrup A (2007) Efficacy and safety of the weight-loss drug rimonabant: a meta-analysis of randomised trials. Lancet 370:1706-1713.

Darlington CL (2003) Dexanabinol: a novel cannabinoid with neuroprotective properties. IDrugs 6:976-979.

Dening TJ, Rao S, Thomas N, Prestidge CA (2016) Oral nanomedicine approaches for the treatment of psychiatric illnesses. J Control Release 223:137-156.

Durmaz R, Ozden H, Kanbak G, Aral E, Arslan OC, Kartkaya K, Uzuner K (2008) The protective effect of dexanabinol (HU-211) on nitric oxide and cysteine protease-mediated neuronal death in focal cerebral ischemia. Neurochem Res 33:1683-1691.

El-Alfy AT, Ivey K, Robinson K, Ahmed S, Radwan M, Slade D, Khan I, ElSohly M, Ross S (2010) Antidepressant-like effect of delta9-tetrahydrocannabinol and other cannabinoids isolated from Cannabis sativa L. Pharmacol Biochem Behav 95:434-442.
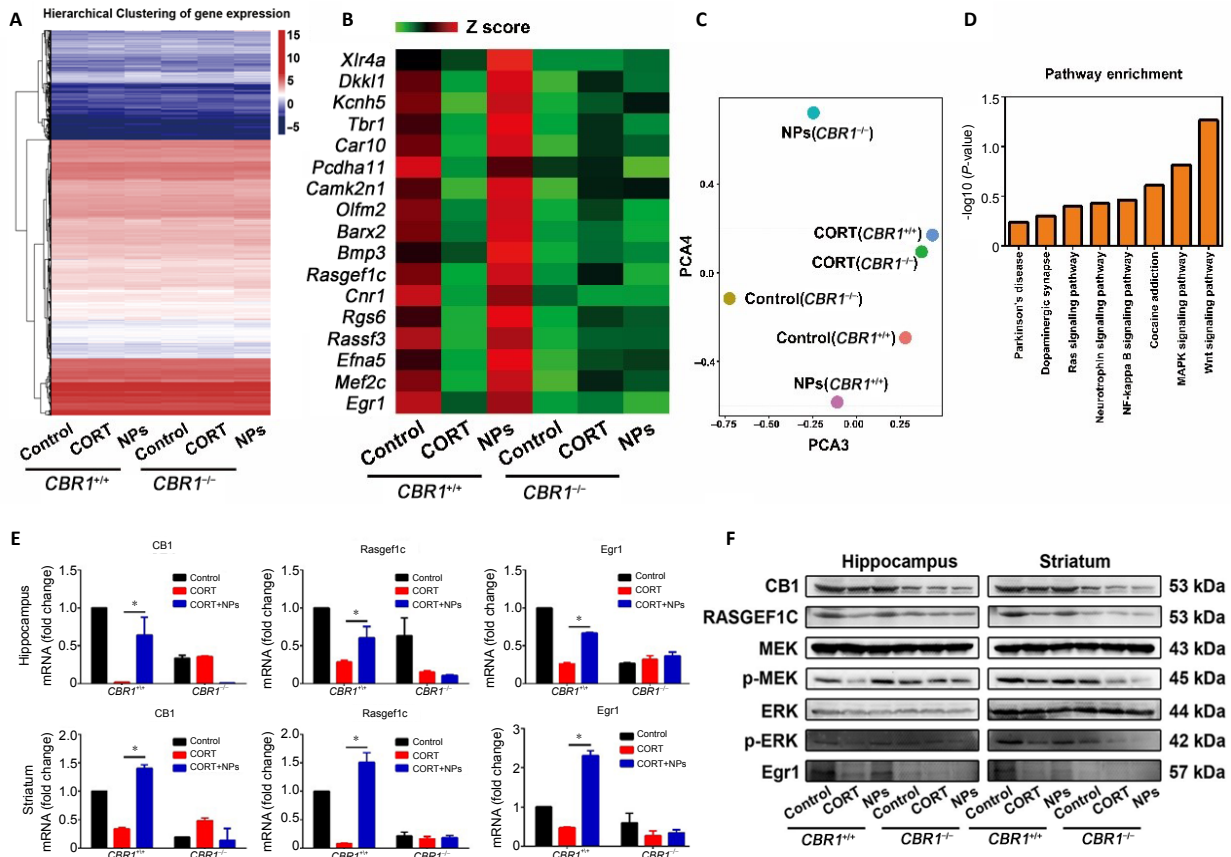
Figure 3 │ Molecular mechanisms of Cur/SLNs-HU-211 on neural differentiation in MDD model mice.
(A) Heatmap representing the global gene-expression pattern of transcription factors in the hippocampus. A total of 505 differentially expressed genes were identified between $CBR1^{+/+}$ CORT + Cur/SLNs-HU-211 and CORT alone. (B) Representative genes are listed, and these 17 genes are mostly neurodevelopment-associated. (C) 2-dimensional principal component analysis (PCA), using genome-wide expression data. (D) Kyoto Encyclopedia of Genes and Genomes pathway analysis between the $CBR1^{+/+}$ CORT + Cur/SLNs-HU-211 and CORT alone groups. The mitogen-activated protein kinase pathway ranked second. (E) Quantitative reverse transcription-polymerase chain reaction analysis of CBR1, Rasgef1c, and Egr1. All groups were normalized against the $CBR1^{+/+}$ control group. Data are presented as the mean ± SD (n = 3/group). *$P < 0.05$ (one-way analysis of variance, followed by the least significant difference test). (F) Western blot images for CBR1, RASGEF1C, MEK, p-MEK, ERK, p-ERK, and Egr1. $CBR1^{-/-}$: Cannabinoid receptor 1 knockout; $CBR1^{+/+}$: wild-type; CORT: corticosterone; Cur/SLNs-HU-211: solid-lipid nanoparticles loaded with curcumin and dexanabinol; Egr1: early growth response 1; ERK: extracellular signal-regulated kinase; MDD: major depressive disorder; MEK: mitogen-activated protein kinase kinase; NPs: nanoparticles loaded with curcumin and dexanabinol (Cur/SLNs-HU-211); p-ERK: phospho-extracellular signal-regulated kinase; p-MEK: phospho-mitogen-activated protein kinase kinase; RASGEF1C: RasGEF domain family member 1C.

Gregus A, Wintink AJ, Davis AC, Kalynchuk LE (2005) Effect of repeated corticosterone injections and restraint stress on anxiety and depression-like behavior in male rats. Behav Brain Res 156:105-114.

Guerzoni LP, Nicolas V, Angelova A (2017) In vitro modulation of TrkB receptor signaling upon sequential delivery of curcumin-DHA loaded carriers towards promoting neuronal survival. Pharm Res 34:492-505.

He X, Zhu Y, Wang M, Jing G, Zhu R, Wang S (2016) Antidepressant effects of curcumin and HU-211 coencapsulated solid lipid nanoparticles against corticosterone-induced cellular and animal models of major depression. Int J Nanomedicine 11:4975-4990.

He X, Yang L, Wang M, Zhuang X, Huang R, Zhu R, Wang S (2017) Targeting the endocannabinoid/CB1 receptor system for treating major depression through antidepressant activities of curcumin and dexanabinol-loaded solid lipid nanoparticles. Cell Physiol Biochem 42:2281-2294.

Hill MN, Carrier EJ, McLaughlin RJ, Morrish AC, Meier SE, Hillard CJ, Gorzalka BB (2008) Regional alterations in the endocannabinoid system in an animal model of depression: effects of concurrent antidepressant treatment. J Neurochem 106:2322-2336.

Hou Z, Zhang J, Yu K, Song F (2020) Irisin ameliorates the postoperative depressive-like behavior by reducing the surface expression of epidermal growth factor receptor in mice. Neurochem Int 135:104705.

Kalani A, Chaturvedi P (2017) Curcumin-primed and curcumin-loaded exosomes: potential neural therapy. Neural Regen Res 12:205-206.

Kroh EM, Parkin RK, Mitchell PS, Tewari M (2010) Analysis of circulating microRNA biomarkers in plasma and serum using quantitative reverse transcription-PCR (qRT-PCR). Methods 50:298-301.

Lakiotaki E, Giaginis C, Tolia M, Alexandrou P, Delladetsima I, Giannopoulou I, Kyrgias G, Patsouris E, Theocharis S (2015) Clinical significance of cannabinoid receptors CB1 and CB2 expression in human malignant and benign thyroid lesions. Biomed Res Int 2015:839403.

Liu MH, Li W, Zheng JJ, Xu YG, He Q, Chen G (2020) Differential neuronal reprogramming induced by NeuroD1 from astrocytes in grey matter versus white matter. Neural Regen Res 15:342-351.

López-Cardona AP, Pérez-Cerezales S, Fernández-González R, Laguna-Barraza R, Pericuesta E, Agirregoitia N, Gutiérrez-Adán A, Agirregoitia E (2017) CB(1) cannabinoid receptor drives oocyte maturation and embryo development via PI3K/Akt and MAPK pathways. FASEB J 31:3372-3382.

Lopresti AL (2017) Curcumin for neuropsychiatric disorders: a review of in vitro, animal and human studies. J Psychopharmacol 31:287-302.

Rakotoarisoa M, Angelova A (2018) Amphiphilic nanocarrier systems for curcumin delivery in neurodegenerative disorders. Medicines (Basel) 5:126.

Rakotoarisoa M, Angelov B, Garamus VM, Angelova A (2019) Curcumin- and fish oil-loaded spongosome and cubosome nanoparticles with neuroprotective potential against H_2O_2-induced oxidative stress in differentiated human SH-SY5Y cells. ACS Omega 4:3061-3073.

Segev A, Rubin AS, Abush H, Richter-Levin G, Akirav I (2014) Cannabinoid receptor activation prevents the effects of chronic mild stress on emotional learning and LTP in a rat model of depression. Neuropsychopharmacology 39:919-933.

Seki K, Yoshida S, Jaiswal MK (2018) Molecular mechanism of noradrenaline during the stress-induced major depressive disorder. Neural Regen Res 13:1159-1169.

Shen CJ, Zheng D, Li KX, Yang JM, Pan HQ, Yu XD, Fu JY, Zhu Y, Sun QX, Tang MY, Zhang Y, Sun P, Xie Y, Duan S, Hu H, Li XM (2019) Cannabinoid CB(1) receptors in the amygdalar cholecystokinin glutamatergic afferents to nucleus accumbens modulate depressive-like behavior. Nat Med 25:337-349.

Si M, Sun Q, Ding H, Cao C, Huang M, Wang Q, Yang H, Yao Y (2020) Melatonin-loaded nanoparticles for enhanced antidepressant effects and HPA hormone modulation. Adv Polym Tech 2020:4789475.

Szczepanik JC, de Almeida GRL, Cunha MP, Dafre AL (2020) Repeated methylglyoxal treatment depletes dopamine in the prefrontal cortex, and causes memory impairment and depressive-like behavior in mice. Neurochem Res 45:354-370.

Wośko S, Serefko A, Szopa A, Wlaź P, Wróbel A, Wlaź A, Górska J, Poleszak E (2018) CB(1) cannabinoid receptor ligands augment the antidepressant-like activity of biometals (magnesium and zinc) in the behavioural tests. J Pharm Pharmacol 70:566-575.

Yamamoto Y, Lee D, Kim Y, Lee B, Seo C, Kawasaki H, Kuroda S, Tanaka-Yamamoto K (2012) Raf kinase inhibitory protein is required for cerebellar long-term synaptic depression by mediating PKC-dependent MAPK activation. J Neurosci 32:14254-14264.

Zhou D, Li Y, Tian T, Quan W, Wang L, Shao Q, Fu LQ, Zhang XH, Wang XY, Zhang H, Ma YM (2017) Role of the endocannabinoid system in the formation and development of depression. Pharmazie 72:435-439.